Visible Light Communications:
Simplified Co-Equalisation of Fast OFDM in a Multiple-Input Multiple-Output Configuration

Paul Anthony Haigh[†], Andrew Burton[‡], Zabih Ghassemlooy[‡] and Izzat Darwazeh[†]

[†]*Communications and Information Systems Group University College London, Gower Street, WC1E 6BT, United Kingdom*
[‡]*Optical Communications Research Group, Northumbria University, Newcastle-upon-Tyne, NE1 8ST, United Kingdom*
{p.haigh; i.darwazeh}@ucl.ac.uk; {andrew2.burton; z.ghasselooy}@northumbria.ac.uk

Abstract—In this paper we experimentally demonstrate, for the first time, a simplified co-equalisation for imaging multiple-input multiple-output based visible light communication systems. We show that in such systems, where all channels have similar magnitude responses, an equaliser trained on a single channel produces coefficients that may be used in the form of a look-up table to equalise the remaining channels without the need for explicit or bespoke training. The system demonstrated is based on the fast-orthogonal frequency division multiplexing based on pulse amplitude modulation scheme to improve the spectral efficiency, where a data rate of 80 Mb/s is achieved using four light-emitting diodes, each of a 4 MHz raw bandwidth. We show that the reported system performance closely matches that of the traditional and more computationally complex system in terms of bit-error rate.

I. Introduction

One of the main research challenges in visible light communications (VLC) is associated with the light-emitting diodes (LEDs), normally consisting of a fast blue-emitting chip and a slow phosphor colour converter, which inhibits the overall transient response of the device, limiting the operating bandwidth (BW) to a few MHz [1]. To overcome this challenge, researchers have turned to high spectral efficiency modulation formats such as orthogonal frequency division multiplexing (OFDM) and carrier-less amplitude and phase modulation (CAP), both of which deliver high data rates [2]. There is an emerging alternative known as fast-OFDM (FOFDM), which was first proposed for wireless systems [3], that has been adopted first in optical fibre systems [4], later in VLC [5, 6] and more recently in 5G Internet-of-Things systems [7]. The fundamental difference between FOFDM and OFDM is that the symbols are modulated using an inverse discrete cosine transform (IDCT) at a symbol spacing of $1/2T$, where T is the symbol period, instead of an inverse fast Fourier transform (IFFT) at $1/T$, thus using half the BW [5]. However, only real-valued (hence one-dimensional) symbol constellation maps may be used. Even so, FOFDM is a potential candidate for VLC since it is inherently real-valued, thus no Hermitian symmetry is required as in OFDM systems. This is highly advantageous because it allows the full use of the electrical spectrum. Furthermore, in [5], we showed that FOFDM offers up to a 3 dB power saving over OFDM in highly band-limited

links, hence in this work we have adopted FOFDM as the preferred modulation format.

Alternatively the link data rates can be increased by means of (*i*) multiple-input multiple-output (MIMO) techniques [8]; and (*ii*) high performance equalisers [9]. The former is readily available in indoor environments where numerous lighting fixtures are installed to provide illumination. In VLC systems, an imaging lens enables channel matrix de-correlation, thus offering effectively line-of-sight paths between the transmitter and receiver with very little inter-channel interference [8]. We adopt an imaging MIMO VLC system in this paper to enable improved transmission speeds. As for equalisers one could use an artificial neural network (ANN), which is normally realised in transversal finite impulse response (FIR) filter form [9]. ANNs offer an outstanding ability to remove inter-symbol interference (ISI) from signals, albeit at the cost of significant computational complexity. In MIMO links, it has been proposed that each link requires an individual equaliser to undo the ISI on each channel due to differing channel responses [10].

In this paper, we propose a 4×4 imaging MIMO VLC system based on FOFDM, which is configured to induce ISI in high frequency subcarriers, and ANN equaliser. We experimentally show for the first time, that it is possible to train an ANN equaliser on the data of a single channel and use the weighted coefficients in a look-up table (LUT) format to equalise the remaining channels. Hence, only a single equaliser training sequence is required where the computational complexity is reduced by four times compared with the system proposed in [10]. We compare the total bit-error rate (BER) performance of the proposed system to a more complex system where each channel has an independent equaliser, with similar BER.

II. Experimental Test Setup

The schematic of the experimental testbed is shown in Fig. 1. The MIMO system is composed of 4 LEDs and 4 photodetectors (PDs), however only two are shown here for clarity. Four independent data streams $\mathbf{D^m} = \left[d_0^m, \ldots d_{L-1}^m \right]$ are generated per channel, where m is the channel number and $L = 2^{13} - 1$ is the length of the pseudorandom binary
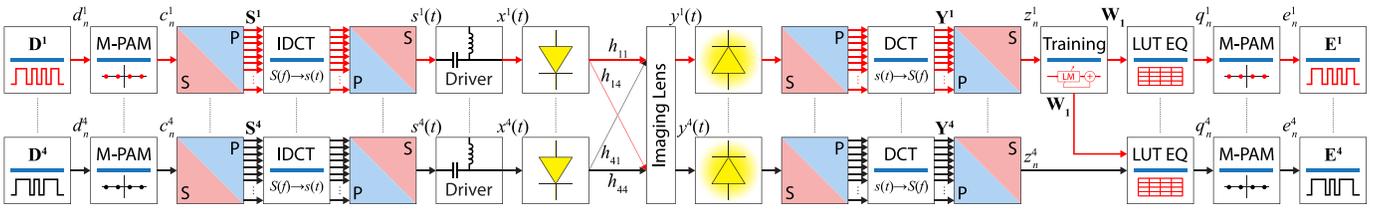
Fig. 1. Simplified block diagram of the proposed system.

sequence. Each data bit is then mapped onto the 4-PAM constellation and converted into N parallel streams for modulation by an IDCT, given by [5]:

$$s^m(t) = \sum_{n=0}^{N-1} w_n c_n^m \cos\left(\frac{\pi n t}{N}\right) \qquad (1)$$

where c_n^m is a 4-PAM symbol modulated onto the nth subcarrier for the mth channel, and N is the total number of subcarriers, which is set to 256 in this work since this gives a good trade-off between complexity and performance [5]. Finally, w_n is a normalisation factor. The serialised output of IDCT $s^m(t)$ is then loaded into a Tektronix 3252C arbitrary function generator (not shown in Fig. 1), which in turn feeds an LED driver. The signal for intensity modulation is $x^m(t) = s^m(t) + I_{DC}$, where I_{DC} is a DC current level set to 350 mA. The LEDs used (Philips Luxeon Rebels) have a BW of ~ 4 MHz/LED, see Fig. 2 where the inset shows the measured magnitudes. Note that the channels have similar responses, both in terms of BW (within 100 kHz variation) and the measured power levels, maximum variation ~ 2.5 dBm. The signal BW is set to 10 MHz, exceeding the system BW, which despite the ISI induced, will result in a gross data rate of 80 Mb/s (4 channels $\times$ 2 bits/symbol $\times$ 10 MHz signal BW).

The transmission distance is set to 2 m and an imaging lens is used for de-correlation of the link, i.e., for resolving the h-matrix and ensuring that only the light from a single transmitter is focused on one of the four PDs at the receiver as in [8]. The optical Rx is composed of silicon PDs (Centronics OSD15-5T with a 15 mm^2 photoactive area), which are reverse biased at 30 V, followed by transimpedance amplifiers (Analog Devices AD8015). The output of each transimpedance amplifier is captured using a real time digital oscilloscope (Keysight DSO9254A) for digitisation prior to offline signal processing. Following digitisation, each signal is converted into a parallel format with $N = 256$ subcarriers prior to DCT transformation and parallel-to-serial conversion.

An example of the received spectrum for channel 1 is shown in Fig. 3, where attenuation >10 dB can be observed at frequencies beyond ~ 8 MHz (i.e. in good agreement with Fig. 2), which introduces ISI. Note that, to compensate for the ISI, equalisers (of different types) are often used and realised as FIR filters. Recent work showed that one of best performing equalisers is the multilayer perceptron-based ANN [9]. ANNs are divided into three layers (i) the input layer, where the symbols are presented to the equaliser; (ii) the hidden layer, where

the processing takes place through neurons, the functional unit of ANNs, which uses an activation function to weigh symbol values based on their ISI contribution; and (iii) the output layer. Their overall operating principles are not detailed here, due to space considerations, but may be found in [9], where each layer is described in detail. Note, every equaliser requires training to be able to estimate the system response for repairing the bit sequence and removing the ISI. In systems such as this one, where no cross talk is present due to the imaging lens [8], an individual equaliser would generally be required for each channel.
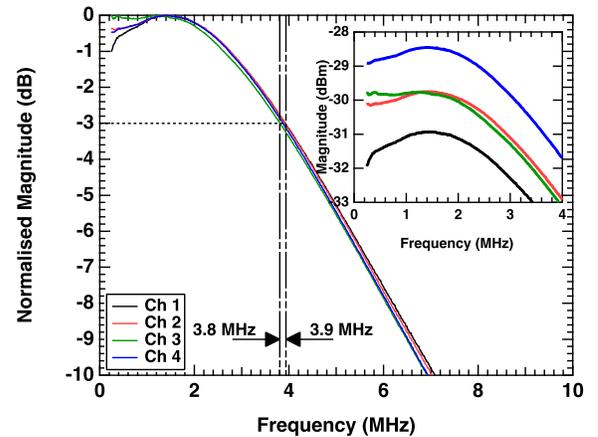

Fig. 2. The normalised end-to-end system frequency responses. The inset shows the measured responses pre-normalisation.
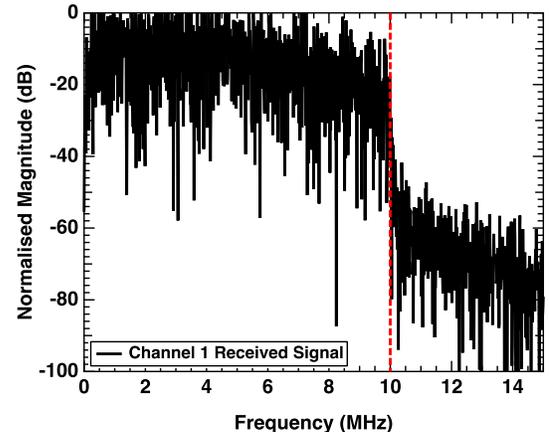

Fig. 3. The measured normalised channel 1 received electrical spectrum.

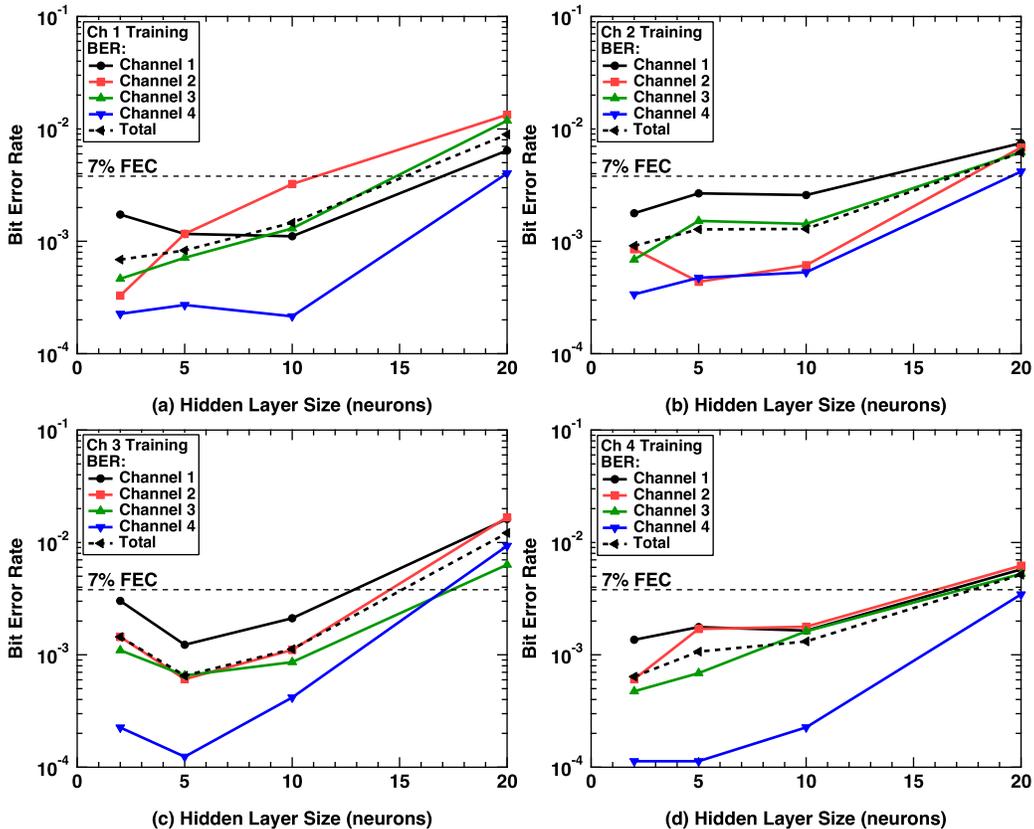While this would be the optimal solution as individual dis-

Fig. 4. The BER as a function of N_t and N_n for a single equaliser trained using data from channels: (a) 1, (b) 2, (c) 3, and (d) 4.

tinctions and imperfections of each channel could be tailored for, this is also the one of the most complex equalisation schemes. Such a high-level of computational complexity is mostly associated with the training sequence, which generally involves at least a single division and numerous multiplications. In this work, we use Levenberg-Marquardt back-propagation training method, which is a popular scheme for equalisation in VLC systems [11]. As for ANN equalisers, their performance is dependent on the number of taps N_t and neurons N_n. It has been noted that selecting Nt and Nn insufficiently or excessively will result in sub-optimal performance or over-training, respectively [12]. Hence, a trade-off between complexity and performance. In this work we select $N_t = N_n = \{2, 5, 10, 20\}$ to illustrate this.

Once the filter coefficients are decided, it is possible that a LUT is able to provide the same functionality. In an imaging MIMO VLC system and in optical wireless communications in general, all channels have approximately equal frequency responses. We postulate that it is possible to train one equaliser on a single arbitrarily selected individual channel and use the resulting coefficients in a direct multiply-and-add LUT format to equalise the remaining channels, thus significantly reducing the computational complexity by a factor of four. We test this hypothesis by sequentially training the equaliser on an individual channel then using the resulting coefficients to equalise the remaining channels using a LUT. We measure

the BER of each channel and the total BER performance. We compare these scenarios with a more conventional system, where each channel has its own equaliser with a high level of complexity.

III. RESULTS

The BER plots as functions of the ANN hidden layer size (i.e., N_t and N_n) for the proposed architecture are shown in Figs. 4(a)—(d). In Fig. 4(a) the BER results are shown for a single equaliser-based system, which is trained on channel 1. Also shown for reference is the 7% forward error correction (FEC) limit as a horizontal dashed line at a BER of 3.8×10^{-3}. As can be observed in Fig. 4(a), following training on the data from channel 1, the best performing channel is channel 4.

The reason for the improved performance observed in channel 4 in comparison to channel 1 is because of the received power level of each channel. With reference to the inset in Fig. 2, for channel 1 the peak measured power level is ~ 2.5 dBm lower than that of channel 4 and hence, channel 4 has a superior signal-to-noise ratio (SNR) and can tolerate less accurate training. This is because the Euclidean distance between symbols is greater. The same effect can be observed in channels 2 and 3, where both offer better BER performance (i.e. steadily increasing) than channel 1 for $N_t = N_n > 5$. The increase in the BER as a function of higher values of N_t and N_n, is due to overfitting and the incorrect ANN-based

estimation of the system frequency response, which leads to errors. The total BER plot shown in Fig. 4(a) represents the ratio of the sum of the errors on each channel to the sum of the total number of transmitted bits, which shows a slow variation up to $N_t = N_n = 10$ and then increases rapidly beyond this value, as expected.

The BER plots for the equaliser trained on channel 2 and with its trained neuron weights used to equalise the other channels are shown in Fig. 4(b). Like the previous case, channel 4 also offers superior BER performance, which closely matches channel 2. For $N_t = N_n = 2$, the BER values are $\sim 10^{-3}$ and 3×10^{-4} for channels 2 and 3, respectively, whereas for $N_t = N_n = 5$ and 10, the BER for both channels is $\sim 5 \times 10^{-4}$. For channels 1 and 3, the BER exceeds these values whilst remaining beneath the FEC limit for $N_t = N_n < 20$. Once more, following the same trend as previously observed, the BER exceeds the FEC limit for $N_t = N_n = 20$, raising to a value within the range of $\sim 4 \times 10^{-3}$ (i.e., channel 4) to $\sim 8 \times 10^{-3}$ (channel 1). In every case we attribute this to overfitting of the training sequence by setting N_t and N_n excessively. Note, the total BER plot follows the same trend previously described, which slowly increases with N_t and N_n.
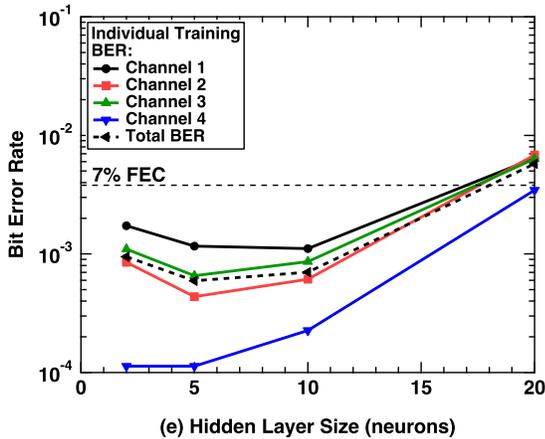

(e) Hidden Layer Size (neurons)

Fig. 5. BER results for channels with their own equalisers.

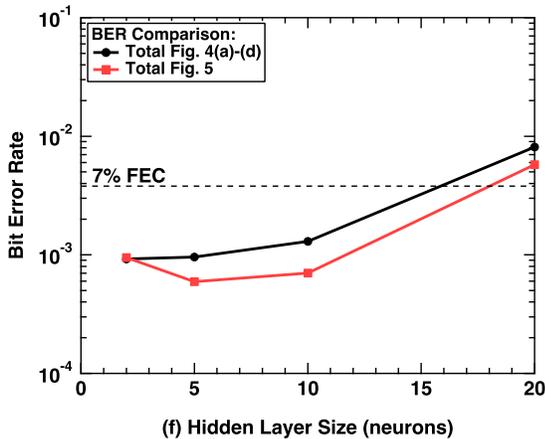(f) Hidden Layer Size (neurons)

Fig. 6. A comparison of BER results for the proposed and conventional cases.

In the next case where the equaliser is trained using channel 3, see Fig. 4(c), the trend observed is slightly different to the previous two cases, as there is a local minimum in the BER profiles for $N_t = N_n = 5$; this is not noticed in the previous plots. This reason for this is attributed to the system frequency responses, see Fig. 2. For channels 1, 2 and 4, a cut-on effect can be observed between DC and ~ 1 MHz, due to the bias-tees used as part of intensity modulation circuitry of the LEDs. For channel 3, this effect is not observed, possibly due to variations in the bias-tee cut-on frequencies. Hence, for $N_t = N_n = 2$ the ANN is not able to correct the additional errors, which are introduced below the frequency of ~ 1 MHz. While for $N_t = N_n > 2$ the ANN does correct the errors associated with lower frequency subcarriers, thus leading to improved BER performance for $N_t = N_n < 20$.

For the final case where the ANN trained on channel 4, the BER performance achieved is the best in comparison to all other cases, see Fig.4(d). This improvement is due to the higher received optical power (higher link SNR), which directly affects the training performance. Therefore, we conclude that the optimal performance will be obtained when the equaliser is trained on the channel with the highest power. In Fig.5, the BER results are presented for each channel with a dedicated equaliser, which match the plots shown in Fig. 4(a)—(d). Finally, in Fig. 6 we show a direct comparison between the total BER of single equalisers (i.e. Fig. 4(a)—(d)) and the individual equalisers (i.e., Fig. 5, with the latter displaying marginally improved performance for $N_t = N_n > 2$. The most important implication of this work is that, similar BER performance can be achieved by adopting the proposed simplified method of training-based on a single channel and using LUTs to equalise the remaining channels. Excluding the case with $N_t = N_n = 20$, which has exceeded the 7% FEC limit for every test, the measured BER results are below this limit, and hence the slight BER penalty observed can be fully accommodated. This is particularly significant since computational complexity is reduced four times, which represents considerable savings when considering training algorithms with divisions and multiplications.

IV. CONCLUSION

In this work we have experimentally demonstrated a simplified co-equalisation technique for the imaging MIMO VLC system with ISI. We showed that, by training a single equaliser based on the data from a single channel, it is possible to use the weight coefficients in a LUT to equalise the remaining channels and therefore achieve improved BER performance, which is comparable to that of a significantly more complex system. The best performance is achieved when the ANN is trained on the signal with the highest power.

ACKNOWLEDGMENT

REFERENCES

[1] T. Koonen, "Indoor optical wireless systems: technology, trends, and applications," *Journal of Lightwave Technology*, vol. 36, no. 8, pp. 1459–1467, 2018.

[2] G. Stepniak, L. Maksymiuk, and J. Siuzdak, "Experimental comparison of PAM, CAP, and DMT modulations in phosphorescent white LED transmission link," *IEEE Photonics Journal*, vol. 7, no. 3, pp. 1–8, 2015.

[3] M. Rodrigues and I. Darwazeh, "Fast OFDM: A proposal for doubling the data rate of OFDM schemes," 2002.

[4] J. Zhao and A. Ellis, "Designs of coherent optical fast OFDM and performance comparison to conventional OFDM," in *Signal Processing in Photonic Communications*. Optical Society of America, 2013, pp. SPT2D–1.

[5] P. A. Haigh and I. Darwazeh, "Visible light communications: Fast-orthogonal frequency division multiplexing in highly bandlimited conditions," in *IEEE/CIC ICCC, 2017*. IEEE, 2017, pp. 1–8.

[6] Y. Shao, Y. Hong, and L.-K. Chen, "On CSI-free linear equalization for optical fast-OFDM over visible light communications," in *Optical Fiber Communication Conference*. Optical Society of America, 2018, pp. M3K–5.

[7] T. Xu and I. Darwazeh, "Non-orthogonal narrowband internet of things: A design for saving bandwidth and doubling the number of connected devices," *IEEE Internet of Things Journal*, 2018.

[8] K. Werfli, P. Chvojka, Z. Ghassemlooy, N. B. Hassan, S. Zvanovec, A. Burton, P. A. Haigh, and M. R. Bhatnagar, "Experimental demonstration of high-speed 4× 4 imaging multi-CAP MIMO visible light communications," *Journal of Lightwave Technology*, vol. 36, no. 10, pp. 1944–1951, 2018.

[9] P. A. Haigh, Z. Ghassemlooy, S. Rajbhandari, I. Papakonstantinou, and W. Popoola, "Visible light communications: 170 Mb/s using an artificial neural network equalizer in a low bandwidth white light configuration," *Journal of lightwave technology*, vol. 32, no. 9, pp. 1807–1813, 2014.

[10] P. A. Haigh, Z. Ghassemlooy, I. Papakonstantinou, F. Tedde, S. F. Tedde, O. Hayden, and S. Rajbhandari, "A MIMO-ANN system for increasing data rates in organic visible light communications systems," in *Communications (ICC), 2013 IEEE International Conference on*. IEEE, 2013, pp. 5322–5327.

[11] P. Jesudhas, M. T. Manry, R. Rawat, and S. Malalur, "Analysis and improvement of multiple optimal learning factors for feed-forward networks," in *The 2011 International Joint Conference on Neural Networks (IJCNN)*. IEEE, 2011, pp. 2593–2600.

[12] T. A. Eriksson, H. Bülow, and A. Leven, "Applying neural networks in optical communication systems: Possible pitfalls," *IEEE Photonics Technology Letters*, vol. 29, no. 23, pp. 2091–2094, 2017.